Modeling Analysis of Platinum-195m for Targeting Individual Blood-Borne Cells in Adjuvant Radioimmunotherapy

John D. Willins and George Sgouros

Department of Medical Physics, Memorial Sloan-Kettering Cancer Center, New York, New York

The inability to eradicate a population of single, isolated, blood-borne tumor cells with the radionuclides currently in use may limit the efficacy of adjuvant radioimmunotherapy. We have examined the possibility of sterilizing single blood-borne cells using surface-bound emitters of Auger and conversion electrons. **Methods:** The number of cell-surface decays required for 99% sterilization was found by using the linear-quadratic model of cell survival (α = 0.3 Gy^{-1}, α/β = 10 Gy) to transform absorbed dose to survival probability. The absorbed dose to the center of the cell was calculated by evaluating the point dose kernel at the cell radius of 6 μm and multiplying it by the number of surface decays. A two-compartment model of whole-body pharmacokinetics was used to obtain the red marrow dose corresponding to a given number of cell-surface decays. **Results:** Platinum-195m ($T_{1/2}$ = 4 days) proves to be a particularly effective radionuclide. The ^{195m}Pt protocol requires 1.2 GBq of injected activity and is calculated to give an average red-marrow dose of 1.23 Gy, well within marrow tolerance. **Conclusion:** Analysis of the targeting efficiency as a function of cell radius reveals that ^{195m}Pt is expected to sterilize cells with radii up to 8 μm without delivering more than 2.5 Gy to red marrow. It also emits photons that are appropriate for external imaging and has been used to study the biodistribution of cisplatin in humans. High-specific activity ^{195m}Pt may be obtained by decay of cyclotron-produced ^{195m}Ir ($T_{1/2}$ = 3.8 hr).

Key Words: radioimmunotherapy; micrometastases; adjuvant therapy; platinum-195m

J Nucl Med 1995; 36:315–319

Experimental and theoretical evidence suggest that radioimmunotherapy (RIT) may be most effective when used in an adjuvant setting to target micrometastases (*1–14*). Prevascular micrometastases and individual blood-borne cells are inherently easier to target than solid tumors since such cells are rapidly accessible to an intravenously administered antibody. A fundamental limitation of adjuvant RIT may be the difficulty of sterilizing single, isolated cells. In a cell cluster, the radiation dose to each cell is enhanced by emissions from adjacent cells; the absence of this "crossfire" dose to an isolated cell makes it, in principle, a much more challenging target (*15,16*). Because of the range-energy characteristics of most currently available radionuclides, their emissions from the cell surface or from the cytosol are generally not effective in eradicating the individual cell.

The low-energy Auger emitter, ^{125}I, whose effectiveness is traditionally associated with the need for intranuclear localization (*17,18*) is a potential exception since it also emits higher energy Auger and conversion electrons. With most radionuclides, however, especially in continuous beta emitters such as ^{131}I, only a small proportion of the energy emitted as electrons from the cell surface is deposited within the nucleus. Although the number of decays on the cell surface could, in principle, be increased to achieve a sterilizing effect with such radionuclides, efficiency is critical because, in practice, the number of available sites and the normal-tissue tolerance (i.e., the red marrow dose) limit the administered activity and consequently the number of decays per cell.

The criteria for identifying optimum radionuclides for adjuvant radioimmunotherapy are completely different from those applied to radioimmunotherapy of solid disease. In solid disease, beta emitters such as ^{32}P, ^{90}Y and ^{188}Re are considered optimal. In contrast, we have undertaken a general analysis of electron-capture (EC) decaying radionuclides for use in RIT against single cells and micrometastases. Radionuclides decaying by EC emit large numbers of low-energy conversion and Auger electrons, many of which have ranges of the order of one cell radius.

As a result of this analysis, we have identified ^{195m}Pt as very promising; its potential for single-cell sterilization is contrasted with that of the familiar radioiodines, ^{123}I, ^{125}I and ^{131}I.

METHODS

We calculated the dose imparted to the center of a spherical cell by a given number of decays on its surface. The cell radius, r, assumed in this study was 6 μm; a range of other radii was also examined. Absorption of radiation dose was described by a point

Received Mar. 23, 1994; revision accepted Jul. 12, 1994.

For correspondence contact: John D. Willins, PhD, Dept. of Medical Physics, Memorial Sloan-Kettering Cancer Center, 1275 York Ave., New York, NY 10021.

For reprints contact: George Sgouros, PhD, Dept. of Medical Physics, Memorial Sloan-Kettering Cancer Center, 1275 York Ave., New York, NY 10021.

TABLE 1
Electron Emissions of ^{195m}Pt Used in Our Dose-Kernel Calculations

Energy, keV	Yield*
0.4	0.87
2	3.22
7	0.81
10	0.52
12	0.01
18	0.69
21	0.66
29	0.21
51	0.17
62	0.01
86	0.12
96	0.04
117	0.64
127	0.20
130	0.07

*Yield is defined as the number of particles per decay. Data were obtained from reference 23. The emissions at 18, 21 and 29 keV give a large dose to the nucleus when originating from the cell surface.

dose kernel k(r), defined as the dose per decay deposited at distance r from a point source in water. Thus, the absorbed dose $D = \tilde{A} \cdot k(6\ \mu m)$, where $\tilde{A}$ is the total number of disintegrations on the cell surface. The dose kernel contains the geometric factor $1/r^2$; the product $r^2\ k(r)$ is known as the scaled dose kernel F(r). The point kernels for ^{123}I, ^{125}I, ^{131}I and ^{195m}Pt were calculated using INKERNEL, a program provided by Dr. Douglas Simpkin, which interpolates Berger's monoenergetic electron point kernels (*19–21*). Tabulated radionuclide emission spectra (*22,23*), including both continuous and discrete electron emissions, were used in computing the point dose kernels. The ^{195m}Pt electron emissions used in our calculations are shown in Table 1.

Given the tumor-cell dose, the probability of cell survival is calculated using the linear-quadratic model, $S = \exp(-\alpha D - \beta D^2)$, where S is the survival probability, D is the absorbed dose and α and β are numerical coefficients. We have used typical tumor-cell values of $\alpha = 0.3\ Gy^{-1}$ and $\alpha/\beta = 10$ Gy. (*24*). The dose which gives 99% sterilization is then 8.36 Gray; 99% sterilization is used as an index for comparing ^{195m}Pt with other radionuclides. An estimate of the patient cure probability may be obtained by raising the single-cell kill probability to the power of the number of tumor cells in the patient. No dose-rate or repopulation effects are incorporated into our model.

To place our results in the context of clinical achievability, we have calculated the red marrow dose corresponding to each tumor-cell dose. This was done by simulating a clinical radioimmunotherapy protocol in which 10 mg (66.7 nmole) of antibody were administered as a bolus to a patient with 10 g (10^{10} isolated cells) of blood-borne tumor (*10,25*). A two-compartment model of whole-body pharmacokinetics yielded the time-varying concentrations of free and bound antibody, and from these the cumulated free and bound activities were computed (*10,25*). The antibody was assumed to distribute uniformly within a 3.8-liter volume, corresponding to the plasma plus the extracellular fluid volumes of liver, spleen and red marrow, which are tissues lacking well-developed capillary basal laminae (*26,27*). This volume was assumed to contain a uniform concentration of readily accessible antigen sites to which the antibody could bind reversibly. The total number of antigen sites, free plus bound, was fixed at 7.5 nmole, corresponding to 4.5×10^5 sites per cell.

In calculating red marrow cumulated activities, the conservative assumption was made that all tumor cells resided within the red-marrow extracellular fluid volume. Average marrow dose was calculated according to the MIRD S-Factor formalism (*28,29*). The S-factors S(rm←rm) and S(rm←tb) (where rm = red marrow, tb = total body) have been calculated for ^{195m}Pt from previously published tables (*30*); the values obtained were 2.0×10^{-8} and 1.7×10^{-10} Gy/MBq-s, respectively.

RESULTS

Table 2 presents the principal results for a cell with a 6 μm radius. The number of cell-surface decays required to give 99% probability of cell sterilization is represented by $\tilde{A}_{99}$. The injected activity required to give 99% sterilization is also listed, as is the corresponding red-marrow dose. The $\tilde{A}_{99}$ is found to be above 20,000 for the radioiodines but only 5,200 for ^{195m}Pt. The red marrow dose is greater than 2.5 Gray for ^{123}I and ^{131}I, making these unlikely candidates for clinical therapy against single cells unless marrow rescue or transplantation is performed. In contrast, ^{195m}Pt gives a marrow dose of 1.23 Gray. The injected activity required to achieve 99% sterilization with ^{195m}Pt is 1.2 GBq, as shown.

In order to determine whether the lethality of ^{195m}Pt is an artifact of choosing cell radius r = 6 μm, we have examined the behavior of $\tilde{A}_{99}$ as a function of r. The surface density of antigen sites is assumed the same for all cell radii; thus the number of sites per cell increases as r^2. The number of cells is assumed to vary as $1/r^2$, so that the systemic num-

TABLE 2
The Number of Cell-Surface Decays Required for 99% Sterilization with ^{123}I, ^{125}I, ^{131}I and ^{195m}Pt

Radionuclide	$T_{1/2}$(days)	$\tilde{A}_{99}$	A_t, GBq	D_{RM}, Gy	E(20–30), keV
^{123}I	0.6	51,000	67.7	3.65	2.9
^{125}I	60.1	23,000	1.59	0.87	8.1
^{131}I	8.0	45,500	6.36	9.32	1.0
^{195m}Pt	4.0	5,200	1.18	1.23	19.4

$T_{1/2}$ is the radionuclide half-life; $\tilde{A}_{99}$ is the number of cell-surface decays required for 99% sterilization; A_t is the corresponding amount of injected activity; D_{RM} is the corresponding red-marrow dose; E(20–30) is the energy released per decay as electrons with energies from 20 to 30 keV.

TABLE 3
The Variation of $\tilde{A}_{99}$ with Cell Radius r

r, μm	$\tilde{A}_{99}$, kBq-s	$\tilde{A}_{Tol}$, kBq-s	$\frac{\tilde{A}_{Tol}}{\tilde{A}_{99}}$
3	1.34	2.66	1.99
4	1.95	4.74	2.43
5	2.96	7.39	2.50
6	5.24	10.6	2.02
7	10.3	14.5	1.41
8	20.0	18.9	0.95
9	36.1	24.0	0.66
10	53.5	29.6	0.55

$\tilde{A}_{Tol}$ is the cell-surface activity corresponding to the red marrow tolerance dose of 2.5 Gy.

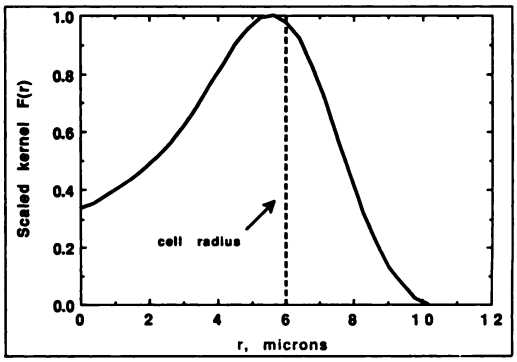

FIGURE 1. The structure of the normalized scaled point kernel F(r) for 21-keV electrons. The dashed line indicates the cell radius assumed in this study. Electrons of this energy are emitted abundantly by ^{195m}Pt (Table 1).

ber of antigen sites is constant at 7.5 nmole. In this case, the red marrow dose is independent of r.

Results with ^{195m}Pt for cell radii from 3 to 10 μm are shown in Table 3. At each radius, we list $\tilde{A}_{99}$, the number of decays giving 99% sterilization; and $\tilde{A}_{Tol}$, the number of decays corresponding to a marrow-tolerance (2.5 Gy) protocol (*31*). The ratio $\tilde{A}_{Tol}/\tilde{A}_{99}$ provides an index of potential effectiveness when treating to marrow tolerance. Values of $\tilde{A}_{Tol}/\tilde{A}_{99} > 1$ indicate that a probability of cell sterilization > 99% may be achieved with a protocol that delivers less than 2.5 Gy to marrow; conversely, values < 1 indicate that 99% sterilization cannot be achieved without excessive marrow toxicity. It is important to note that $\tilde{A}_{Tol}/\tilde{A}_{99}$ is a more biologically relevant quantity than an absorbed-dose therapeutic ratio (D_{tumor}/D_{rm}) because it refers directly to tumor-cell control and normal tissue complication. Table 3 shows that $\tilde{A}_{Tol}/\tilde{A}_{99}$ does not simply fall with increasing r, but rather has a broad maximum near r = 5 μm. The ratio is >1 for all cell radii less than 8 μm. At these radii, the number of cell surface decays required to achieve 99% sterilization is still lower than the values provided in Table 2 for the three radioiodines. The greater killing efficiency of ^{195m}Pt per cell-surface disintegration is particularly important for antibodies that bind to antigen that is not highly expressed on tumor cell-surfaces (the CD33 antigen in leukemia, for example (*32*)). Platinum-195-labeled antibody is therefore expected to sterilize single cells while sparing red marrow for a broad range of cell sizes and at relatively low levels of antigen expression.

To investigate why ^{195m}Pt appears to be relatively lethal to the single cell over a wide range of radii, we have examined the structure of the point dose kernel at various electron energies. Figure 1 shows the (normalized) scaled point kernel F(r) for 21-keV electrons. A strong peak appears whose maximum lies at 5.6 μm. Therefore, a 21 keV emitter on the surface of a cell with a 6 μm radius would be comparatively well positioned to deliver dose to the center. However, the full kernel k(r) contains the factor $1/r^2$, hence a smaller distance from the emitter is generally more advantageous. Figure 2 displays F(r), and $k(r) = F(r)/r^2$ on the same scale. We note that k(r) is falling only slowly in the neighborhood of 3–6 μm, meaning that the entire nucleus would be expected to receive a large dose. As Table 1 shows, ^{195m}Pt has strong emissions of electrons at 21 keV, as well as at 18 and 29 keV.

DISCUSSION

The advantages of targeting micrometastatic rather than solid disease with radioimmunotherapy have been established primarily on theoretical grounds (*1–6,8,10,12–14*). Radioimmunotherapy directed towards eradication of micrometastases has not been investigated clinically, however. The difficulty of assessing efficacy rapidly and in a small patient population; the reluctance to administer radiolabeled antibody to patients who may not have overt evidence of disease; and the recognition that currently available radionuclides are not effective for sterilizing isolated single cells, have all contributed to the slow acceptance of micrometastasis-targeted radioimmunotherapy. The latter, in particular, is potentially a fundamental limitation of adjuvant radioimmunotherapy when it is used as the only adjuvant treatment modality.

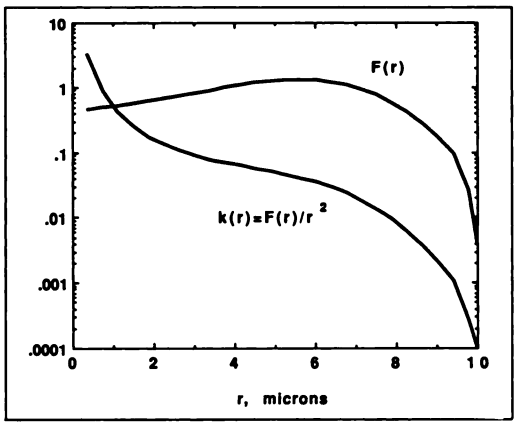

FIGURE 2. The scaled kernel F(r) and the product $k(r) = F(r)/r^2$, for 21-keV electrons. F is normalized as in Figure 1.

In this work, we have identified a radionuclide, ^{195m}Pt, that exhibits potential for eradicating individual blood-borne cells without exceeding red marrow tolerance. A number of investigators have evaluated various radionuclides for solid and micrometastatic disease (*15,33–38*). We have focused on targeting single, isolated cells that are within the initial distribution volume of intravenously-administered, intact antibody. By incorporating a two-compartment model of antibody pharmacokinetics (*10,25*), as well as the linear-quadratic model of cell survival (*39*), we have included red marrow dose and tumor cell control probability in our evaluation.

Platinum-195m has other desirable characteristics. It decays with a half-life of 4.02 days and emits photons, in the energy range 65–130 keV, which may be imaged. The biodistribution of platinum-containing compounds has been studied both in humans and experimental animals. In particular, the chemotherapeutic agent, cisplatin (*cis*-diaminedichloroplatinum (II)), an inorganic planar coordination complex for platinum, has been studied extensively (*40–47*). Because a potential approach to antibody labeling with ^{195m}Pt would be via attachment to cisplatin, the biodistribution of this drug may be relevant to understanding the fate of the radiolabel following its dissociation from the antibody. Correspondingly, ^{195m}Pt-cisplatin-labeled antibody that is internalized may exhibit a compounded chemotherapeutic and radiation-induced cytotoxic effect (*48*).

Although ^{195m}Pt is available for cisplatin tracer studies, its current mode of production, ^{194}Pt(n,γ), yields a very low specific activity product ($\approx$ 30 MBq/mg platinum) rendering it unusable for radioimmunotherapy. We have identified two alternative approaches to its production: (1) cyclotron production of iridium-195m (^{195m}Ir, $T_{1/2}$ = 3.8 hr), followed by decay to ^{195m}Pt; and (2) nuclear reactor production of osmium-195 (^{195}Os) which decays to ^{195m}Ir with a 6.5-min half-life. Both methods are generator systems which should yield a very high specific activity product. Iridium-195m may be produced in a cyclotron via the ^{198}Pt(p,α) or ^{192}Os(α,p) reactions. At a proton energy of 20 MeV, the (p,α) reaction has a cross-section of approximately 3 mb and is rising with proton energy (Hill JC, *personal communication*) (*49*). We are currently examining potential approaches to the production of high-specific activity ^{195m}Pt.

It is important to note that our analysis does not include the effects of dose-rate and tumor cell proliferation. Given the rapid accessibility of blood-borne tumor cells and the short half-life (4 days) of ^{195m}Pt relative to characteristic doubling times (5–30 days) of solid-tumor cells, these omissions will not have a great impact on the advantage of ^{195m}Pt for targeting single cells originating from solid disease. In targeting very rapidly proliferating, single-cell disease such as leukemia, however, such considerations will become more influential (*50*).

Using a set of selection criteria that incorporate radionuclide emissions, half-life, the dose to red marrow and tumor cell control probability, we have identified ^{195m}Pt as a promising radionuclide for targeting isolated single cells with radioimmunotherapy. This radionuclide also has the desirable properties of emitting photons appropriate for imaging; of having a chelate already available (i.e., cisplatin) that may be used to bind to the antibody and of having been studied extensively in humans and animals. Although low-specific activity ^{195m}Pt is available, high-specific activity ^{195m}Pt that is necessary for radioimmunotherapy requires an investigation of several alternative production schemes.

ACKNOWLEDGMENTS

The authors thank Drs. Ronald Finn, John Humm, Steven Larson and C. Clifton Ling for their comments and suggestions. They are also grateful for the assistance, in identifying the pertinent literature and providing information on nuclear reaction cross sections and resonant energies, of Dr. Frank S. Rotondo of the Physics Department at Yale University and of Dr. John C. Hill of the Physics and Astronomy Department at Iowa State University.

REFERENCES

1. Bigler RE, Zanzonico PB, Cosma M, Sgouros G. Adjuvant radioimmunotherapy for micrometastases: a strategy for cancer cure. In: Srivastava SC, ed. *Radiolabeled antibodies for imaging and therapy.* New York: Plenum Press; 1988:409–429.
2. Wheldon TE, O'Donoghue JA, Hilditch TE, Barrett A. Strategies for systemic radiotherapy of micrometastases using antibody-targeted ^{131}I. *Radiother Oncol* 1988;11:133–142.
3. Jain RK, Baxter LT. Mechanisms of heterogeneous distribution of monoclonal antibodies and other macromolecules in tumors: significance of elevated interstitial pressure. *Can Res* 1988;48:7022–7032.
4. Bigler RE, Zanzonico PB, Sgouros G, Strauss A, Godwin TA. Feasibility dosimetry for radioimmunotherapy for micrometastases (RIMM) [Abstract]. *J Nucl Med* 1990;31:788.
5. van Osdol W, Fujimori K, Weinstein JN. An analysis of monoclonal antibody distribution in microscopic tumor nodules: consequences of a "binding site barrier." *Can Res* 1991;51:4776–4784.
6. O'Donoghue JA. Optimal scheduling of biologically targeted radiotherapy and total body irradiation with bone marrow rescue for the treatment of systemic malignant disease. *Int J Radiat Oncol Biol Phys* 1991;21:1587–1594.
7. Sharkey RM, Weadock KS, Natale A, et al. Successful radioimmunotherapy for lung metastasis of human colonic cancer in nude mice. *J Natl Cancer Inst* 1991;83:627–632.
8. Weinstein JN, van Osdol W. Early intervention in cancer using monoclonal antibodies and other biological ligands: micropharmacology and the "binding site barrier." *Can Res* 1992;52(suppl):2747S–2752S.
9. Blumenthal RD, Sharkey RM, Haywood L, et al. Targeted therapy of athymic mice bearing GW-39 human colonic cancer micrometastases with I-131-labeled monoclonal antibodies. *Cancer Res* 1992;52:6036–6044.
10. Sgouros G. Plasmapheresis in radioimmunotherapy of micrometastases: a mathematical modeling and dosimetrical analysis. *J Nucl Med* 1992;33:2167–2179.
11. Amin AE, Wheldon TE, O'Donoghue JA, Barrett A. Radiobiological modeling of combined targeted ^{131}I therapy and total body irradiation for treatment of disseminated tumors of differing radiosensitivity. *Int J Radiat Oncol Biol Phys* 1993;27:323–330.
12. Willins J, Sgouros G. Improving the targeting of blood-borne micrometastases in radioimmunotherapy: a mathematical analysis of sequential cold and hot antibody infusions [Abstract]. *Med Phys* 1993;20:865.
13. Willins JD, Sgouros G. Predicting the effectiveness of radioimmunotherapy against micrometastases: kinetic modeling, marrow dosimetry and tumor control probability [Abstract]. *J Nucl Med* 1994;35:123P.
14. Sgouros G, Yorke ED, Willins JD, Ling CC. Radioimmunotherapy of micrometastases: theoretical evaluation of adjuvant treatment [Abstract]. *J Nucl Med* 1994;35:161P.
15. Humm JL. Dosimetric aspects of radiolabeled antibodies for tumor therapy. *J Nucl Med* 1986;27:1490–1497.

16. Goddu SM, Dandamudi RV, Howell RW. Multicellular dosimetry for micrometastases: dependence of self-dose versus cross-dose to cell nuclei on type and energy of radiation and subcellular distribution of radionuclides. *J Nucl Med* 1994;35:521–530.
17. Kassis AI, Howell RW, Sastry KSR, Adelstein SJ. Positional effects of Auger decays in mammalian cells in culture. In: Baverstock KF, Charlton DE, eds. *DNA damage by Auger emitters.* London: Taylor and Francis; 1988:1–14.
18. Kassis AI, Makrigiorgos GM, Adelstein SJ. Dosimetric considerations and therapeutic potential of Auger electron emitters. In: Adelstein SJ, Kassis AI, Burt RW, eds. *Frontiers in nuclear medicine: dosimetry of administered radionuclides, symposium proceedings, Washington DC, 1989.* Washington DC: American College of Nuclear Physicians; 1990:257–274.
19. Simpkin DJ, Mackie TR. EGS4 Monte Carlo determination of the beta dose kernel in water. *Med Phys* 1990;17:179–186.
20. Berger MJ. Beta-ray dosimetry calculations with the use of point kernels. In: Cloutier RJ, Edwards CL, Snyder WS, eds. *Medical radionuclides: radiation dose and effects. Proceedings of a symposium held at the Oak Ridge Associated Universities.* U.S. Atomic Energy Commission Report Conf-691212. Washington, DC; 1970:63–86.
21. Berger MJ. Improved pont kernels for electron and beta-ray dosimetry. In: *Center for radiation research,* U.S. Department of Commerce, Washington, DC: *NBSIR;*1973:73–107.
22. Browne E, Firestone RB. *Table of radioactive isotopes.* In: Shirley VS, ed. New York: John Wiley and Sons: 1986:195.
23. Weber DA, Eckerman KF, Dillman LT, Ryman JC. *MIRD: radionuclide and decay schemes.* New York: Society of Nuclear Medicine; 1989:348–349.
24. Ling CC. Permanent implants using ^{198}Au, ^{103}Pd and ^{125}I: radiobiological considerations based on the linear quadratic model. *Int J Radiat Oncol Biol Phys* 1992;23:1–7.
25. Sgouros G, Graham MC, Divgi CR, Larson SM, Scheinberg DA. Modeling and dosimetry of monoclonal antibody M195 (anti-CD33) in acute myelogenous leukemia. *J Nucl Med* 1993;34:422–430.
26. Renkin EM. Multiple pathways of capillary permeability. *Circ Res* 1977;41:735–743.
27. Zamboni L, Pease DC. The vascular bed of red bone marrow. *J Ultrastructure Res* 1961;5:65–85.
28. Snyder WS, Ford MR, Warner GG, Watson SB. "S," absorbed dose per unit cumulated activity for selected radionuclides and organs. *MIRD pamphlet no. 11, revised.* New York: Society of Nuclear Medicine; 1975.
29. Loevinger R, Budinger TF, Watson EE. *MIRD primer for absorbed dose calculations.* New York: Society of Nuclear Medicine; 1989.
30. Snyder WS, Ford MR, Warner GG. Estimates of specific absorbed fractions for photon sources uniformly distributed in various organs of a heterogeneous phantom. *MIRD pamphlet no. 5, revised.* New York: Society of Nuclear Medicine; 1976.
31. Bentel GC, Nelson CE, Noell KT. *Treatment planning and dose calculation in radiation oncology.* New York: Pergamon Press; 1989:4–5.
32. Tanimoto M, Scheinberg DA, Cordon-Cardo C, Huie D, Clarkson BD, Old LJ. Restricted expression of an early myeloid and monocytic cell surface antigen defined by monoclonal antibody M195. *Leukemia* 1989;3:339–348.
33. Wessels BW, Rogus RD. Radionuclide selection and model absorbed dose calculations for radiolabeled tumor associated antibodies. *Med Phys* 1984;11:638–645.
34. Howell RW, Rao DV. Macroscopic dosimetry for radioimmunotherapy: nonuniform activity distributions in solid tumors. *Med Phys* 1989;16:66–74.
35. Humm JL, Cobb LM. Nonuniformity of tumor dose in radioimmunotherapy. *J Nucl Med* 1990;31:75–83.
36. Yorke ED, Beaumier PL, Wessels BW, Fritzberg AR, Morgan AC. Optimal antibody-radionuclide combinations for clinical radioimmunotherapy: a predictive model based on mouse pharmacokinetics. *Nucl Med Biol* 1991;18:827–835.
37. Rao DV, Howell RW. Time-dose-fractionation in radioimmunotherapy: Implications for selecting radionuclides. *J Nucl Med* 1993;34:1801–1810.
38. Mausner LF, Srivastava SC. Selection of radionuclides for radioimmunotherapy. *Med Phys* 1993;20(part 2):503–509.
39. Fowler JF. The linear-quadratic formula and progress in fractionated radiotherapy. *Br J Radiol* 1989;62:679–694.
40. Lange RC, Spencer RP, Harder HC. The antitumor agent cis-Pt$(NH_3)_2Cl_2$: distribution studies and dose calculations for ^{193m}Pt and ^{195m}Pt. *J Nucl Med* 1973;14:191–195.
41. Smith PHS, Taylor DM. Distribution and retention of the anti-tumor agent platinum-195m cis-di-chlorodiammineplatinum(II) in man. *J Nucl Med* 1974;15:349–351.
42. Wolf W, Manaka RC. Synthesis and distribution of Pt-195m cis-dicholordiammine platinum (II). *J Clin Hematol Oncol* 1977;7:79–95.
43. Manaka RC, Wolf W. Radio-pharmacokinetic studies with platinum-195m labeled cis-platin [Abstract]. *J Nucl Med* 1978;19:732.
44. Hoeschele JD, Butler TA, Roberts JA. Microscale synthesis and biodistribution of Pt-195m-labeled cis-dichlorodiammineplatinum(ii), cis-DDP. *Proceedings Second International Symposium on Radiopharmaceuticals* 1979; Seattle, WA.
45. Hoeschele JD, Butler TA, Roberts JA. Correlations of physico-chemical and biological properties with in vivo biodistribution data for platinum-195m-labeled chlorammineplatinum(II) complexes. *Inorganic Chem Biol Med* 1980;140:181–208.
46. Benard P, Desplanches G, Macquet JP, Simon J. Whole-body autoradiographic study of the distribution of ^{195m}Pt in healthy and tumor-bearing mice treated with labeled cisplatin. *Cancer Treat Rep* 1983;67:457–466.
47. Shani J, Bertram J, Russell C, et al. Noninvasive monitoring of drug biodistribution and metabolism: studies with intraarterial ^{195m}Pt cisplatin in humans. *Cancer Res* 1989;49:1877–1881.
48. Howell RW, Kassis AI, Adelstein SJ, et al. Auger electron cascades of ^{195m}Pt: track structure in liquid water and radiotoxicity of ^{195m}Pt labeled trans-platinum (II) in mammalian cells. *Radiat Res* 1994;140:55–62.
49. Fulmer CB, Goodman CD. (p,alpha) reactions induced by protons in the energy range of 9.5–23 MeV. *Phys Rev* 1960;117:1339.
50. Sgouros G, Scheinberg DA. The treatment of leukemia with radiolabeled monoclonal antibodies. In: Rosen ST, Kuzel TM, eds. *Immunoconjugate therapy of hematologic malignancies.* New York: Kluwer Academic Press; 1993:23–64.